Adsorption Kinetics of an Engineered Gold Binding Peptide by Surface Plasmon Resonance Spectroscopy and a Quartz Crystal Microbalance

Candan Tamerler,[†,‡] Ersin Emre Oren,[†] Memed Duman,[†] Eswaranand Venkatasubramanian,[†,§] and Mehmet Sarikaya*[,†,||]

Material Science and Engineering, Department of Chemistry, and Chemical Engineering, University of Washington, Seattle, Washington 98195, and Molecular Biology and Genetics, Istanbul Technical University, Istanbul, Turkey 80626

Received March 13, 2006. In Final Form: June 16, 2006

The adsorption kinetics of an engineered gold binding peptide on gold surface was studied by using both quartz crystal microbalance (QCM) and surface plasmon resonance (SPR) spectroscopy systems. The gold binding peptide was originally selected as a 14-amino acid sequence by cell surface display and then engineered to have a 3-repeat form (3R-GBP1) with improved binding characteristics. Both sets of adsorption data for 3R-GBP1 were fit to Langmuir models to extract kinetics and thermodynamics parameters. In SPR, the adsorption onto the surface shows a biexponential behavior and this is explained as the effect of bimodal surface topology of the polycrystalline gold substrate on 3R-GBP1 binding. Depending on the concentration of the peptide, a preferential adsorption on the surface takes place with different energy levels. The kinetic parameters (e.g., $K_{eq} \sim 10^7\ M^{-1}$) and the binding energy (∼−8.0 kcal/mol) are comparable to synthetic-based self-assembled monolayers. The results demonstrate the potential utilization of genetically engineered inorganic surface-specific peptides as molecular substrates due to their binding specificity, stability, and functionality in an aqueous-based environment.

Introduction

Molecular recognition, binding, and self-assembly properties of proteins are the key concepts in molecular biomimetics.[1,2] Many sequences specific to metals (Au, Ag, Pt),[1,3,4] oxides (ZnO, Cu_2O, $CaCO_3$),[5,6] and semiconductors (CdS, ZnS)[7,8] have been selected using *in vivo* combinatorial biology, e.g., either phage or cell surface display, techniques. Although many of the selected peptides have been demonstrated for their potential use in materials assembly, formation, and growth modification of inorganics, these results have been achieved without the knowledge of the quantitative nature of the interactions between the peptide and the inorganic. One reason for this lack of understanding stems from the limited experiments that have so far been carried out toward this goal.[9,10] The heterogeneity of the inorganic substrate at the atomic, crystallographic, and nanometer scales adds another complexity to the understanding of peptide−inorganic binding mechanism(s). In addition, modeling studies, using, e.g., molecular dynamics, have also been limited and, so far, only confined to the idealized surfaces.[11,12] Clearly a detailed analysis of the binding strategies relying on shape complementarities as well as the physical and chemical interactions is needed for the robust design of hybrid materials exhibiting controlled topology and composition.[9] Furthermore, the adsorption characteristics of the inorganic-binding peptides are necessary for practical applications that would involve proteins or their conjugates as molecular templates. Therefore, the knowledge of kinetics and thermodynamics of biospecific interactions is essential for developing an understanding of the molecular basis of such events. Further progress in the understanding of the inorganic specific peptide adsorption is highly dependent on reliable measurement techniques that can produce rich and accurate information in terms of the strength, kinetics, and specificity of the binding processes.[9]

We have adapted both quartz crystal microbalance (QCM)[13−16] and surface plasmon resonance (SPR) spectroscopy[17−20] techniques to assess quantitatively the binding of an inorganic-specific peptide on a solid surface. Both of the techniques used are sensitive to adsorption and desorption of molecular species on solid substrates in aqueous solutions and have been used fre-

* To whom correspondence should be addressed. E-mail: sarikaya@u.washington.edu. Fax: (+1) 206 543 3100.

† Material Science and Engineering, University of Washington.

‡ Molecular Biology and Genetics, Istanbul Technical University.

§ Department of Chemistry, University of Washington.

|| Chemical Engineering, University of Washington.

(1) Sarikaya, M.; Tamerler, C.; Jen, A. Y.; Schulten, K.; Baneyx, F. *Nat. Mater.* **2003**, *2*, 577−585.

(2) Kriplani, U.; Kay, B. K. *Curr. Opin. Biotechnol.* **2005**, *16*, 470−475.

(3) Brown, S. *Nat. Biotechnol.* **1997**, *15*, 269−272.

(4) Naik, R. R.; Stringer, S. J.; Agarwal, G.; Jones, S. E.; Stone, M. O. *Nat. Mater.* **2002**, *1*, 169−172.

(5) Thai, C. K.; Dai, H. X.; Sastry, M. S. R.; Sarikaya, M.; Schwartz, D. T.; Baneyx, F. *Biotechnol. Bioeng.* **2004**, *87*, 129−137.

(6) Gaskin, D. J. H.; Starck, K.; Vulfson, E. N. *Biotechnol. Lett.* **2000**, *22*, 1211−1216.

(7) Lee, S. W.; Mao, C. B.; Flynn, C. E.; Belcher, A. M. *Science* **2002**, *296*, 892−895.

(8) Peelle, B. R.; Krauland, E. M.; Wittrup, K. D.; Belcher A. M. *Acta Biomater.* **2005**, *1*, 145−154.

(9) Sarikaya, M.; Tamerler, C.; Schwartz, D. T.; Baneyx, F. *Annu. Rev. Mater. Res.* **2004**, *34*, 373−478.

(10) Sano, K. I.; Sasaki, H.; Shiba, K. *Langmuir* **2005**, *21*, 3090−3095.

(11) Braun, R.; Sarikaya, M.; Schulten, K. S. *J. Biomater. Sci.* **2002**, *13*, 747−758.

(12) Oren, E. E.; Tamerler, C.; Sarikaya, M. *Nano Lett.* **2005**, *5*, 415−419.

(13) Höök, F.; Rodahl, M.; Brzezinski, P.; Kasemo, B. *Langmuir* **1998**, *14*, 729−734.

(14) Murray, B. S.; Deshaires, C. *J. Colloid Interface Sci.* **2000**, *227*, 32−4.

(15) Marxer, C. G.; Coen, A. C.; Schlapbach, L. *J. Colloid Interface Sci.* **2003**, *261*, 291−298.

(16) Roach, P.; Farrar, D.; Perry, C. C. *J. Am. Chem. Soc.* **2005**, *127*, 8168−8173.

(17) O'Shannessy, D.; Brighan-Burke, M.; Soncson, K. K.; Hensley, P.; Brooks, I. *Anal. Biochem.* **1993**, *212*, 457−468.

(18) Green, R. J.; Davies, J.; Davies, M. C.; Roberts, C. J.; Tendler, S. J. B. *Biomaterials* **1997**, *18*, 405−413.

(19) Sigal, G. B.; Bamdad, C.; Barberis, A.; Strominger, J.; Whitesides, G. M. *Anal. Chem.* **1996**, *68*, 490−497.

(20) Singh, N.; Husson, S. M. *Biomacromolecules* **2005**, *6*, 9−13.

10.1021/la0606897 CCC: $33.50
Published on Web 08/03/2006

quently.[15,16,20,21] The binding processes could be studied under conditions of peptide selection or application that can easily be controlled via the manipulation of the solution characteristics. For a proof-of-principle demonstration, we used a gold-binding peptide sequence and analyzed its adsorption characteristics on the metallic gold surfaces. Gold-binding peptides, originally selected by cell surface display, are one of the first examples of genetically engineered peptides for inorganics (GEPI).[3,9,22] They were screened via random peptide libraries expressed on the outer surface of *Escherichia coli* as part of the maltodextrin porin, LamB protein. Among the identified peptides, we used the engineered form of GBP1 (MHGKTQATSGTIQS) on the basis of our previous studies that the strong binding property is presented by a three repeat of the original sequence (3R-GBP1). Our preliminary modeling studies also supported the repeating nature of the molecular structure, i.e., an antiparallel β-sheet structure of 3R-GBP1 recognizing the gold surface.[11] The motif does not contain any cysteine residue, which has an −SH group, the linker that is known to bind strongly to gold in synthetic molecules containing thiols that form the basis of self-assembled monolayers (SAM).[23−25]

QCM is used in studying adsorption both in solution and in gas phases (thickness monitoring) of various molecules including SAM-based molecular constructs and proteins.[13−16] In a QCM, quartz crystal is mechanically excited into a resonance by applying an alternating potential across two conducting films deposited on either side of the quartz crystal. The frequency of this oscillation is sensitive to the amount of adsorbed materials on the crystal surface and can be used to monitor the deposition of thin-film materials or adsorption of molecules. Surface plasmon resonance spectroscopy (SPR) is also frequently used to study biomolecular adsorption in solution.[26,27] It is widely used to obtain quantitative binding[20,28] of biological molecules and to study their kinetics of adsorption.[21,29] The technique is based on the effect of the collective excitation of the electrons at the metal−dielectric interface on the wavelength shift of the reflected light from a prism. This shift is affected by the adsorbed molecules on the surface of the metal of the prism causing a change in the refractive index, or the dielectric constant, of the system. Similar to QCM, SPR probes adsorption behavior and is sensitive to sub-nanometer level molecular coverage.

SPR and QCM measurements have many similarities in terms of measuring adsorbed molecules on the surface of a substrate, e.g., metal.[30] Therefore, one would expect these two methods, when used together, to be redundant in studying the adsorption of the same molecule binding to the same material. However, each method measures different physical phenomena. While both measure frequency change in response to the accumulation of the molecule on the surface, SPR is sensitive to the optical properties of the adsorbent and sensitive to the coverage as well as the amount of the molecule. QCM is a mechanical measurement technique and detects the amount (mass) of the molecule whether covering the surface or nonuniformly accumulating on it.[31] Therefore, we have carried out our experiments without knowing whether there may be some differences between the kinetics measured by the two techniques. The GBP1 represents a new class of molecules, i.e., inorganic-specific peptides, binding to a bare material surface, without any linker. Our purpose in carrying out the measurements with the two techniques was to establish each technique's validity and applicability to the binding of an engineered peptide on an inorganic surface. These studies are expected to pave the way to perform similar binding studies with other peptides and their interactions with the relevant materials.

In this paper, we report the binding characteristics of an engineered gold binding peptide (i.e., 3R-GBP1) on metallic gold surfaces using both of the spectroscopic approaches and compare the results. To analyze the results, we applied Langmuir models to adsorption data to extract the kinetics and thermodynamics parameters of the peptide binding. Since the best fit to the adsorption of GBP1 determined via the SPR showed a biexponential behavior, we, therefore, developed a corresponding kinetics for the SPR data and proposed that the two simultaneously occurring binding reactions take place on the gold surface that could be described with a bimodal adsorption, each with a different energy. The results presented here are the first detailed report on the adsorption kinetics of inorganic binding peptides and may be used as a general baseline for the utility of these peptides as potential molecular linkers in directed-assembled systems in nanobiotechnology, surface functionalization, biocompatibility, and soft lithography.[1,25,32]

Materials and Methods

Peptide, Buffer, and Solutions. The solutions containing the synthesized peptide were prepared under various concentrations (0.5, 1, 1.5, 3, 4, 5 μg/mL) and pH values (3.02, 7.52, 9.80, 10.93) in 10 mM phosphate buffer (3:1 K_2HPO_4−KH_2PO_4) containing 100 mM KCl. Concentrated HCl and NaOH were used to equilibrate the desired pH of the 3R-GBP1 solution. Nanopure milli Q water was used for preparing all the solutions unless stated otherwise.

AFM Measurements. Large (~1 μm diameter), atomically flat Au(111)-oriented gold substrates were purchased from Molecular Imaging Corp. (Tempe, AZ). The Au(111) substrates of 5×5 mm^2 surface area were dipped into a solution containing the desired concentration of 3R-GBP1 solution for 20 min. The substrates were then washed in the buffer, rinsed with DI water, and dried with pure nitrogen before examining by AFM. A Digital Instruments Multimode Nanoscope III scanning probe microscope was used to scan the surface to examine assembly of 3R-GBP1. All of the imaging was carried out under tapping mode, with 512×512 data acquisitions at a scan speed of 0.8 Hz at room temperature in air with a scan area of 2×2 μm. The oxide-sharpened silicon nitride tips were used. Supplier-provided mathematical software was employed for extracting quantitative data, such as surface roughness profiles, from the AFM images.

QCM Experiments. AT cut QCM electrodes with a fundamental resonant frequency of 10 MHz were obtained from International Crystal Manufacturing Co. (Oklahoma City, OK). The crystals were coated on both sides with 100-Å chromium and 1000 Å gold. The crystal surfaces were optically polished. The diameter of the crystals and electrodes used were 8.8 and 5.0 mm, respectively. The oscillation electronic circuit is a typical Collpits oscillator, which has a buffer amplifier. A 12 V dc was applied to the oscillator circuit to drive the crystal, and the frequency was measured with a Hewlett-Packard

(21) Calonder, C.; Van Tassel, P. R. *Langmuir* **2001**, *17*, 4392−4395.
(22) Brown, S.; Sarikaya, M.; Johnson, E. *J. Mol. Biol.* **2000**, *299*, 725−732.
(23) Bain, C. D.; Whitesides, G. M. *J. Am. Chem. Soc.* **1989**, *111*, 1, 321−335.
(24) Kafer, D.; Witte, G.; Cyganik, P.; Terfort, A.; Woll, C. *J. Am. Chem. Soc.* **2006**, *128*, 1723−1732.
(25) Love, J. C.; Estroff, L. A.; Kriebel, J. K.; Nuzzo, R. G.; Whitesides, G. M. *Chem Rev.* **2005**, *105*, 1103−1169.
(26) Petoral, R. M.; Uvdal, K. *Colloids Surf., B* **2002**, *25*, 335−346.
(27) Beccati, D.; Halkes, K. M.; Batema, G. M.; Guillena, G.; de Souza, A. C.; van Koten, G.; Kamerling J. P. *Chembiochem* **2005**, *6*, 1196−1203.
(28) Furuya, M.; Haramura, M.; Tanaka, A. *Bioorg. Med. Chem.* **2006**, *14*, 537−543.
(29) Jung, L. S.; Nelson, K. E.; Stayton, P. S.; Campbell, C. T. *Langmuir* **2000**, *16*, 9421−9432.
(30) Laschitsch, A.; Menges, B.; Johannsman, D. *Appl. Phys. Lett.* **2000**, *77*, 2252−2254.
(31) Bailey, L. E.; Kambhampati, D.; Kanazawa, K. K.; Knoll, W.; Frank, C. W. *Langmuir* **2002**, *18*, 479−489.
(32) Davis, F.; Higon, S. P. J. *Biosens. Bioelectron.* **2005**, *21*, 1−20.

frequency counter (model No. 53131A, 225 Hz Universal Counter, Agilent Technologies).

After the crystal was mounted in the cell, the crystals with the gold electrode were first cleaned with 1:3 (v/v) 30% H_2O_2/H_2SO_4, "piranha solution", for 5 min at room temperature and then rinsed with Milli-Q water for 2 min. (***Caution!*** *Piranha solution must be handled with care; it is extremely oxidizing, reacts violently with organics, and should only be stored in loosely tightened containers to avoid pressure buildup.*) The crystals were used immediately after they were dried with high-purity nitrogen gas. To establish a stable baseline, a sufficient amount of buffer solution was introduced into the cell before adding the peptide. The frequency change of the crystal in pure buffer solution was recorded for 30−60 min. After this, desired amount of 3R-GBP1 was introduced into the cell and the frequency change was recorded continuously.

SPR Experiments. The SPR measurements were made with a dual channel instrument (Kretschmann configuration) developed by the Radio Engineering Institute, Czech Republic. It is a generic instrument consisting of a polychromatic light source (ocean optics LS1) coupled with an optical fiber and an Ocean Optics SD 2000 detector. It has 2 angular arms, one of which houses the source and the other the detector. These arms are movable so as to obtain desired angle of incidence. In the middle, there is goniometer stage. The flow cell is housed on the goniometer and consists of a PTFE cell with a Mylar gasket, the thickness of which determines the volume of the cell. The light coming through the fiber strikes the prism at an angle of 66°. The instrument can detect changes in refractive index of the order of 0.0001. The prism and the substrate are made of BK7 glass ($n_e = 1.518\ 72$), and they were coupled together using Cargille (code 1248) immersion oil ($n_d = 1.5150$). The flow cell is pressed against the slide where it is held in place by a clamp.

The SPR substrates were prepared by e-beam evaporation with 48 nm gold layer with 2 nm titanium as adhesion layer. Prior to deposition the slides were cleaned with piranha solution, rinsed thoroughly with DI water, and then dried with nitrogen gas. Before the experiments were carried out, the slides were again cleaned with a basic solution of hydrogen peroxide (H_2O_2:NH_4OH:H_2O = 1:1:5), washed thoroughly with water, and dried in nitrogen gas. The slides were then immersed in buffer solution overnight or until water completely wets the gold surface (e.g., >3 h immersion provides good results). The slide was then dried with nitrogen gas and immediately used for the experiments.

The data were collected using WinSpectral 1.03, the software that was supplied along with the instrument. The software measures the normalized spectrum (dip) at regular intervals, and the dip is then fit with a fourth order polynomial for generating the metric sensogram as a function of time. All measurements were carried out at 27-(±0.1) °C, achieved by housing the whole setup inside a temperature-controlled incubator (VWR Scientific products). During the experiments, solutions were pumped through the flow cell using two peristaltic pumps (Instech Labs) and the inputs were routed through a 6-port valve (Upchurch Scientific) so as to allow rapid switching between solutions. The solutions were pumped at a rate of 80 μL/min. A baseline was first established by pumping buffer, and next the port was switched to peptide solution; following the saturation of the peptide, buffer was pumped once again to monitor the desorption behavior.

Results and Discussion

The 3R-GBP1 adsorption was studied using AFM for different concentration ranges to analyze the monolayer formation of the peptide on the gold surface. Figure 1 shows some examples of the AFM images recorded after the binding at two different concentrations of 3R-GBP1, 0.5 and 5 μg/mL, on the Au(111) surface. Here, the line profiles recorded over parallel domains have a ~1 nm height difference between the peptide regions and the substrate bare surface. This value is equivalent to monolayer thickness of the peptide on the basis of the modeling of 3R-GBP1 forming an antiparallel β-sheet structure.[11] On the basis of the AFM analysis, therefore, we studied the binding characterization of the peptide via QCM and SPR between the peptide concentrations values of 0.5 and 4.0 μg/mL, where it forms a monolayer.

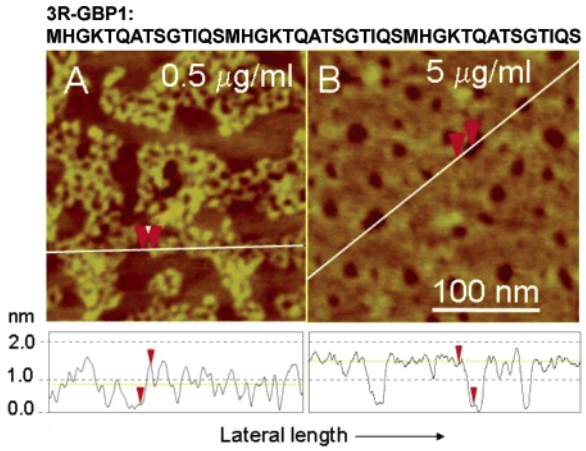

Figure 1. (A) and (B) are AFM images showing partial coverage of 3R-GBP1 on textured Au(111) at 0.5 and 5 μg/mL concentrations, respectively. The line profiles indicate monolayer molecular film formation in both cases. The amino acid sequence of the 3R-GBP1 is given at the top.

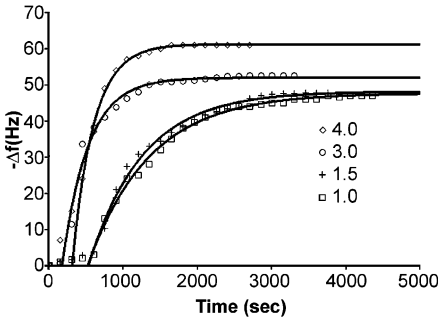

Figure 2. Frequency shift of adsorbed 3R-GBP1 on Au electrode (polycrystalline) for various concentrations carried out by QCM. The fits correspond to Langmuir adsorption isotherms at the relevant peptide concentrations.

QCM Studies. The 3R-GBP1 adsorption was performed on gold-coated quartz crystal electrode, the adsorption times varied to achieve stabilization of frequency, indicating that the system reached the equilibrium. In Figure 2, we see the frequency plots of different peptide concentrations over time. We used a Langmuir isotherm to deduce the kinetics of the adsorption by 3R-GBP1. The Langmuir is the most commonly used isotherm describing monolayer adsorption process by assuming that the number of adsorption sites are fixed and that the adsorption process is reversible.[33] The rate of surface reaction governed by Langmuir isotherms is given by:

$$\frac{d\theta}{dt} = k_a(1 - \theta)C - k_d\theta \qquad (1)$$

where, θ is the fraction of surface covered, C is the 3R-GBP1 concentration, and k_a and k_d are the association and dissociation constants, respectively. The time evolution of the monolayer formation can be obtained by the integration of eq 1 and is given by

(33) Karpovich, D. S.; Blanchard, G. J. *Langmuir* **1994**, *10*, 3315−3322.

$$\theta(t) = \frac{C}{C + (k_d/k_a)}[1 - \exp(-(k_a C + k_d)t)] \quad (2)$$

Substitution of the expressions, $k_{obs} = k_a C + k_d$ and $\theta(\infty) = C/[C + (k_d/k_a)]$ gives

$$\theta(t - t_o) = \theta(\infty)[1 - \exp(-k_{obs}(t - t_o))] \quad (3)$$

The maximum initial rate of monolayer formation is not reached immediately upon injection of 3R-GBP1 solution. Depending on the volume and the concentration of the injected peptide solution, it may take up to several minutes to achieve the maximum adsorption rate because of the limitations inherent to the mixing of the 3R-GBP1 solution and the buffer. To eliminate this mixing effect in eq 3, the variable t in eq 2 is modified with $t - t_o$. Equation 3 can, then, be rewritten in terms of the measured frequency difference, Δf, assuming that there is a linear relation between these two quantities, namely $\Delta f(t) = \alpha\theta(t)$, where α is the proportionality constant:

$$\Delta f(t - t_o) = \Delta f(\infty)[1 - \exp(-k_{obs}(t - t_o))] \quad (4)$$

The parameters of eq 4 are optimized by using a nonlinear optimization algorithm such as the Levenberg−Marquardt method.[34] The fit lines and the experimental data points are in good agreement as shown in Figure 2.

In Table 1, we present $\Delta f(\infty)$ and k_{obs} values, for which the Levenberg−Marquardt method converges, at different 3R-GBP1 concentrations. Using the relationship of $k_{obs} = k_a C + k_d$, we plot the concentration dependence of k_{obs} for 3R-GBP1 and from the best-fit line. As a result, we obtain the value of k_a from the slope and that of k_d from the intercept of the best fit. The values of k_a and k_d are calculated as 3.49×10^3 M^{-1} s^{-1} and 3.12×10^{-4} s^{-1}, respectively. Using these data, the equilibrium constant $K_{eq} = k_a/k_d$ for the formation of the 3R-GBP1/Au complex can be estimated as 1.12×10^7 M^{-1}. We also like to get a quantitative value for the binding energy that reflects the affinity of the 3R-GBP1 to gold surface. For this we use the relationship $\Delta G_{ads} = -RT \ln K_{eq}C$. The standard Gibbs free energy of adsorption (molarity representation) of the 3R-GBP1 monolayer, therefore, is found as − 9.68 kcal/mol directly from the equilibrium constant by choosing 1 M as a standard state for the concentration. When this free energy and the equilibrium constant are compared with those of the existing SAMs on gold surfaces,[24,33] it can be seen that the values of 3R-GBP1 appear to be about the same order of magnitude. Therefore, 3R-GBP1 would be a viable alternative to many of these nonspecific molecules and can also potentially be utilized as a molecular linker as a utility in bionanotechnology.

We next studied the steady-state fractional coverage of the gold surface, $\theta(\infty)$, which is given by

$$\theta(\infty) = \frac{C}{C + K_{eq}^{-1}} \quad (5)$$

The fractional coverage values calculated for the 3R-GBP1/Au system using eq 5 are given in Table 2. Within the 1.0−4.0 μg/mL range of the peptide concentration studied, the measured steady-state coverage in QCM is 64% for the lowest concentration and 87% for the highest one.

SPR Studies. We next performed SPR experiments to determine the kinetic parameters independently and also to compare these to the results of the binding kinetics determined by QCM. For the SPR studies of 3R-GBP1 binding on gold film, all the experimental conditions were kept similar to those in the QCM experiments except that the solution containing the peptides was released into the SPR chamber via a fluid cell with a predetermined optimum flow rate. During the runs, the peptide was pumped until a steady SPR signal was attained; after this point, the buffer was pumped out to wash off any nonspecifically bound peptides on the substrate. A rapid adsorption of the peptide onto the sensor surface was observed which corresponds to a sharp increase in the SPR shift. The sensograms show an increase in the rate of adsorption with an increase in the peptide concentration, an effect that is more pronounced for higher concentration runs (Figure 4). No significant desorption was observed during our experiments. A majority of common immobilization techniques for protein attachments on solid surfaces utilize either nonspecific adsorption or surface functionalization that allow a desired reaction with certain groups exposed on the proteins of interest.[35,36] Here, since 3R-GBP1 was originally selected to bind specifically to gold surface, it is not surprising to see that engineered form also binds to the surface and more tightly, exhibiting a very low desorption behavior. It is possible, therefore, that the peptide/inorganic interaction is through a molecular recognition of gold surface by the engineered 3R-GBP1, providing a stable and high-affinity binding.

While the QCM data could be explained by a simple exponential fit, this is not the case for the peptide adsorption data obtained

Table 1. $\Delta f(\infty)$ and k_{obs} Values Determined from the Raw QCM Data as a Function of 3R-GBP1 Concentration

3R-GBP1 concn			
M	μg/mL	$\Delta f(\infty)$ (Hz)	k_{obs} (s^{-1})
2.32×10^{-7}	1.0	47.63	1.20
3.49×10^{-7}	1.5	48.10	1.37
6.97×10^{-7}	3.0	51.87	2.89
9.29×10^{-7}	4.0	61.17	3.48

Table 2. Fractional Surface Coverage as a Function of 3R-GBP1 Concentration via QCM

3R-GBP1 concn		
M	μg/mL	$\theta(\infty)$
2.32×10^{-7}	1.0	0.72
3.49×10^{-7}	1.5	0.80
6.97×10^{-7}	3.0	0.89
9.29×10^{-7}	4.0	0.91

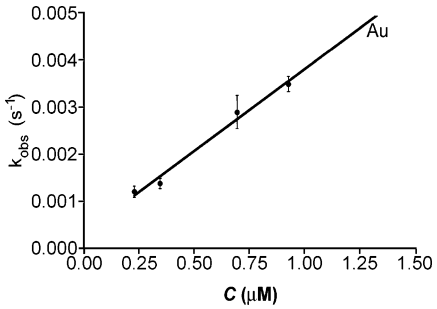

Figure 3. Concentration dependence of k_{obs} for the QCM adsorption data based on the Langmuir model.

(34) Marquardt, D. *SIAM J. Appl. Math.* **1963**, *11*, 431−441.

(35) Bornschever, U. T. *Angew. Chem., Int. Ed.* **2003**, *42*, 3336−3337.

(36) Tomizaki, K.; Usui, K.; Mihara, H. *ChemBioChem* **2005**, *6*, 782−799.

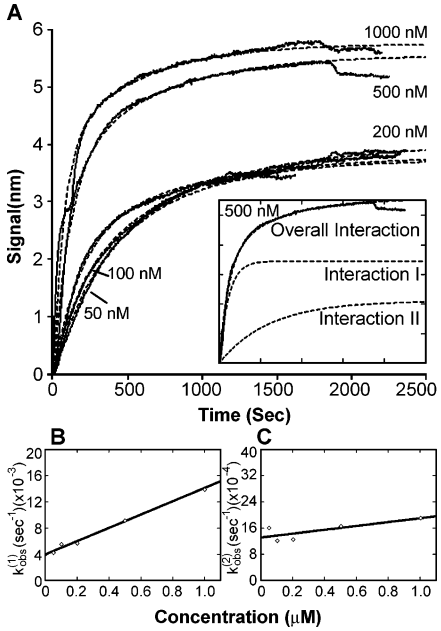

Figure 4. (A) SPR analysis of 3R-GBP1 over a concentration range and the biexponential fits of Langmuir adsorption isotherms to the raw experimental data. The inset shows the model of the two types of adsorption of the molecule that are taking place simultaneously on the surface as well as their total. The concentration dependence of k_{obs} for the two simultaneous reactions are in (B) for $k_{obs}^{(1)}$ and (C) for $k_{obs}^{(2)}$.

by SPR for the adsorption of 3R-GBP1 on gold. For the analysis of peptide adsorption data measured by SPR, we found that the data could be best represented by two separate exponential functions or a biexponential Langmuir model. The use of a biexponential model to describe the behavior of adsorption obtained by SPR results in two different observed rate constants $k_{obs}^{(1)}$ and $k_{obs}^{(2)}$.

In the literature, SPR is used to monitor the kinetic behavior of molecules adsorbed either directly on the SPR substrate (e.g. alkanethiol adsorption on bare gold)[33] or interaction of biomolecules (e.g. DNA, protein, or cell adhesion) onto an already functionalized SPR substrate (e.g., alkanethiol-functionalized gold).[37] In the former case, adsorption behavior of many thiol-based molecules interacting directly to gold surface, measured by SPR, follows a simple exponential trend.[33,38,39] For the latter case, however, there are reports showing biexponential behavior.[40−43] In this latter case, however, there is no common agreement on the meaning of the two rate constants obtained, especially the slower rate.[42] In these literature studies, it has been reported that the fast reaction rate corresponds to the binding interaction of the molecule of interest and gives more insight in the kinetic process.[40,44] The slower reaction rate has been suggested to arise either from steric hindrance[45] or diffusion limitations.[46,47] In general, however, this slow rate has also been attributed to the intrinsic problems associated with the biosensor method, hence, providing little or no information about the intrinsic biomolecular interaction with the substrate.[40,41] In our case of 3R-GBP1 adsorption on bare gold, one possible explanation of the biexponential behavior could be that there are two different types of regions on the gold surface. These two regions on the surface may constitute two structural domains with different defect density or topography, such as grain boundaries versus crystallographically smooth regions of the grains. Assuming that the 3R-GBP1 binding kinetics on these two different domains on the surface could be fairly independent from each other, then the total fraction of surface coverage may be given as $\theta_{obs}(t) = x_1\theta_1(t) + x_2\theta_2(t)$. Here, $x_1 + x_2 = 1$, where x_1 and x_2 denote the fractions of the sites that are responsible in resulting different adsorption behaviors in terms of thermodynamics and kinetics parameters. These include standard Gibbs free energies, entropies, and, finally, the activation energies. These parameters manifest themselves in terms of two different $k_{obs}^{(1)}$ and $k_{obs}^{(2)}$ constants and their concentration and temperature dependencies. For the present case, we may write

$$\theta_{obs}(t) = x_1\theta_1(t) + x_2\theta_2(t) = x_1\theta_1(\infty)(1 - \exp(-k_{obs}^{(1)}t)) + x_2\theta_2(\infty)(1 - \exp(-k_{obs}^{(2)}t)) \quad (6)$$

where, the observed rate constants are functions of association and dissociation rate constants, k_a and k_d, respectively, and are given by $k_{obs}^{(1)} = k_a^{(1)}C + k_d^{(1)}$ and $k_{obs}^{(2)} = k_a^{(2)}C + k_d^{(2)}$.

Equation 6 can be translated into the experimentally measurable quantity Signal (*Sig*), i.e., the shift in the SPR wavelength measured in nanometers. This can be accomplished by utilizing a linear relation $Sig_{obs}(t) = \alpha\theta_{obs}(t)$. Therefore, we may write

$$Sig_{obs}(t) = Sig_1(t) + Sig_2(t) = Sig_1(\infty)(1 - \exp(-k_{obs}^{(1)}t)) + Sig_2(\infty)(1 - \exp(-k_{obs}^{(2)}t)) \quad (7)$$

where, $Sig_i(t) = x_i\alpha\theta_i(t)$.

The parameters of eq 7 are optimized by using the same nonlinear optimization algorithm described for the QCM case. As a result of this process, the obtained model fits and data points are provided in Figure 4A. We achieved model fits with high accuracy on the basis of the assumption that 3R-GBP1 might involve two different simultaneous binding processes occurring on the surface of gold. The $Sig_1(\infty)$, $k_{obs}^{(1)}$ and $Sig_2(\infty)$, $k_{obs}^{(2)}$ values for two independent interactions are given in Table 3. On the basis of these analyses, we next plotted the concentration dependence of $k_{obs}^{(1)}$ and $k_{obs}^{(2)}$ for 3R-GBP1 (Figure 4B,C). The values of $k_a^{(1)}$ and $k_d^{(1)}$ are calculated to be $1.01 \times 10^4\ M^{-1}\ s^{-1}$ and $3.95 \times 10^{-3}\ s^{-1}$ for the first binding mechanism, and $k_a^{(2)}$ and $k_d^{(2)}$ are calculated to be $5.87 \times 10^2\ M^{-1}\ s^{-1}$ and $1.30 \times 10^{-3}\ s^{-1}$ for the second binding mechanism, respectively. The striking feature in these two binding processes is the difference between the two k_a values, i.e., about 20 times difference, while the k_d values are very similar, i.e., only a 3-fold difference. This may mean that while two, a slower and a faster, adsorption processes are taking place, there is only a slower, perhaps single, desorption rate of 3R-GBP1 from the surface. The corresponding equilibrium constants, $K_{eq}^{(1)}$ and $K_{eq}^{(2)}$, for the formation of the GBP/Au complex are estimated as $2.54 \times 10^6\ M^{-1}$ and $4.51 \times 10^5\ M^{-1}$, respectively, for the first and the second mechanisms. In summary, although the overall values of kinetics parameters determined

(37) Mrksich, M. *Cell. Mol. Life Sci.* **1998**, *54*, 653−662.
(38) Jung, L. S.; Campbell, C. T. *J. Phys. Chem. B* **2000**, *B104*, 11168−11178.
(39) Schessler, H. M.; Karpovich, D. S.; Blanchard, G. J. *J. Am. Chem. Soc.* **1996**, *118*, 9645−9651.
(40) Edwards, P. R.; Robin, J. *Anal. Biochem.* **1997**, *246*, 1−6.
(41) Henry, M. R.; Stevens, P. W.; Sun, J.; Kelso, D. M. *Anal. Biochem.* **1999**, *276*, 204−214.
(42) O'Shannessy, D. J.; Winzor, D. J. *Anal. Biochem.* **1996**, *236*, 275−283.
(43) Chan, V.; Graves, D. J.; McKenzie, S. E. *Biophys. J.* **1995**, *69*, 2243−2253.
(44) Corr, M.; Slanetz, A. E.; Boyd, L. F.; Jelonek, M. T.; Khilko, S.; Al-Ramadi, B. K.; Kim, Y. S.; Maher, S. E.; Bothwell, A. L. M.; Marguiles, D. H. *Science* **1994**, *265*, 946−949.
(45) Edwards, P. R.; Lowe, P. A.; Leatherbarrow, R. J. *J. Mol. Recognit.* **1997**, *10*, 128−134.
(46) Glaser, R. W. *Anal. Biochem.* **1993**, *213*, 152−161.
(47) Schuck, P. *Biophys. J.* **1996**, *70*, 1230−1249.

Table 3. $Sig_1(\infty)$, $k_{obs}^{(1)}$ and $Sig_2(\infty)$, $k_{obs}^{(2)}$ Values Determined from Raw SPR Data as a Function of 3R-GBP1 Concentration

3R-GBP1 concn					
nM	μg/mL	$Sig_1(\infty)$	$k_{obs}^{(1)}$	$Sig_2(\infty)$	$k_{obs}^{(2)}$
50	0.22	1.23	4.20×10^{-3}	2.50	1.60×10^{-3}
100	0.43	2.30	5.50×10^{-3}	1.50	1.20×10^{-3}
200	0.86	1.50	5.60×10^{-3}	2.50	1.25×10^{-3}
500	2.15	3.45	9.10×10^{-3}	2.10	1.65×10^{-3}
1000	4.30	3.90	1.40×10^{-2}	1.85	1.90×10^{-3}

Table 4. Fractional Surface Coverage as a Function of 3R-GBP1 Concentration for the First and the Second Binding Mechanisms for SPR Studies and the Ratio of Two Domains on the Au Surface

3R-GBP1 concn		fractional surf coverage		surf area ratio	
nM	μg/mL	surf I $\theta(\infty)$	surf II $\theta(\infty)$	% surf I	% surf II
50	0.22	0.11	0.02	8.8	91.2
100	0.43	0.20	0.04	24.6	75.4
200	0.86	0.34	0.08	12.8	87.2
500	2.15	0.56	0.18	35.0	65.0
1000	4.30	0.71	0.31	47.7	52.3

using QCM and SPR fall within a similar range, one can obtain a more detailed analysis on concurrently occurring binding processes using the SPR because of its molecular sensitivity. The results of binding kinetics and strength obtained from both systems demonstrate that 3R-GBP1 could be an alternative, for certain applications, to the existing thiol-based synthetic molecules that self-assemble on gold surfaces and are used as linkers for variety of synthetic and biological molecules.[24,36,48]

Using the data discussed above, we also calculated the standard Gibbs free energy of adsorption (molarity representation) of the 3R-GBP1 monolayer for the two independent reactions as −8.797 and −7.765 kcal/mol, respectively. Here, we used eq 5 and chose 1 M as a standard state for the concentration. It is known that the thiol-based molecules that are frequently used in SAM applications have energies of adsorption in the −5 to −10 kcal/mol range. For example, the free energy of adsorption of 1-octadecanethiol is −5.6(0.2) and −5.5(0.4) kcal/mol in *n*-hexane and in cyclohexane solvents, respectively.[33,39] On the basis of this particular example, we see that the energy of adsorption of 3R-GBP1 is lower than that for the thiol-based system on gold. In addition, the adsorption is measured in water-based solvent for the peptide providing biology-friendly conditions. Since 3R-GBP1 was originally specifically selected to bind to gold, it, therefore, provides the desired specific affinity for this metal compared to others, e.g., platinum, to which it binds weakly.[49] Here, in describing the binding energy, we intentionally chose not to use the term "free energy" since its determination, based on the equilibrium constant, is an approximation in the absence of activity measurements. To find the binding energy, one would need to carry out binding experiments at different temperatures. Regardless of the assumptions, the energy obtained is directly related to the free energy and is a measure of the binding of the peptide. Therefore, we prefer to call it binding energy in lieu of the free energy.

The fractional coverage values calculated for the 3R-GBP1/Au system using eq 6 are given in Table 4. From the equilibrium surface coverage, $\theta_1(\infty)$ *and* $\theta_2(\infty)$, and the measured $Sig_1(\infty)$ and $Sig_2(\infty)$ values, the surface characteristic of Au substrates may be calculated using the following formula given in eq 8. Here the values can easily be obtained using the proportionality

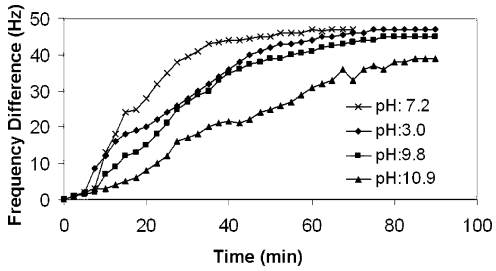

Figure 5. pH effect for 3R-GBP1 adsorption on gold substrate (1 μg/mL) determined by the QCM technique.

relations among measured quantities and the fractional coverages. Hence, we may write:

$$x_1 = \frac{Sig_1(\infty)\theta_2(\infty)}{Sig_1(\infty)\theta_2(\infty) + Sig_2(\infty)\theta_1(\infty)}$$

$$x_2 = \frac{Sig_2(\infty)\theta_1(\infty)}{Sig_1(\infty)\theta_2(\infty) + Sig_2(\infty)\theta_1(\infty)} \quad (8)$$

These relations give the fractions of the two domains (or regions) on the tested substrates where each acts independently and affects the adsorption kinetics differently. On the basis of this assumption, Table 4 also gives the relative percentages of these two domains that are active in the adsorption of the peptide at various concentrations. For example, at low concentration, we see one of the domains is more favorable in the adsorption process, resulting in ∼90% coverage compared to ∼10%. As the concentration increases, however, both of the domains, provide equally favorable conditions for 3R-GBP1 adsorption.

Finally, we studied the adsorption of 3R-GBP1 under a wide range of pH conditions (3−11) using the QCM to assess the adsorption behavior of the peptide and its pH sensitivity. The results are displayed in Figure 5. Although somewhat lower adsorption was observed in either of the extreme conditions, surprisingly, the binding of the peptide was not significantly different from those observed under neutral pH conditions. This result suggests that the peptide probably retains its structural conformation over a large pH range, which then results in tight binding. This pH insensitivity to binding as a result of the high conformational stability and, hence, the strong binding for the peptide on to gold could be a major advantage for the practical utility of this GEPI under specific applications.

(48) McGovern, M. E.; Thompson, J. *Can. J. Chem.* **1999**, *77*, 1678−1689.
(49) Tamerler, C.; Duman, M.; Oren, E. E.; Gungormus, M.; Xiong, X.; Kacar, T.; Parviz, A. B.; Sarikaya, M. *Small*, in press.

Currently thiols and silanes are being widely used as linkers and immobilizing agents for biological and functional synthetic molecules on to gold (or silver) and oxides (e.g., silica glass), respectively.[36,39,48] In this report, we demonstrated the quantification of the kinetics of adsorption of an inorganic binding peptide, namely a gold-binding peptide. The binding of the peptide is fairly tight (comparable to thiol-based systems), and the process of binding is fast (completing the 90% coverage within 20 min), taking place under aqueous conditions compatible with biological environments. Although we do not know the exact mechanism of GBP binding to the gold, here we speculate that the polar groups in the 3-repeat sequence, e.g., hydroxyl and amine, exposed via the M, K, T, Q, and S residues, may play an important role as a group rather than as individual amino acids in providing a cumulative binding. As is well-known in the protein structure literature, it is not just the chemical but also the physical structure of the protein (i.e., its 3-dimensional conformation in space) that equally significantly affects its binding and molecular recognition characteristics. Gold-binding peptide and, in general, genetically selected or engineered peptides with specific binding affinity to metals and oxides may find utility in nano- and nanobiotechnologies as novel agents of surface functionalization.

Conclusions

Among the biomolecules, proteins are the most promising ones for practical applications because of their capability of carrying vast range of information and due to their recognition, binding, and assembly characteristics. Consequently, inorganic surface specific proteins are becoming key molecules in the engineering of bioinspired and biomimetic materials fabrication and organization.[1,2,7] Recent introduction of genetic methods and bioinformatics concepts into designing, tailoring, and manipulating inorganic binding peptides is resulting in more and varied sequences.[9] It is clear that, for their robust use and wide range of applicability, the evaluation of peptide binding kinetics is essential. In this work, we report, for the first time, the adsorption kinetics of an engineered inorganic binding peptide via two different methods, quartz crystal microbalance (QCM) and surface plasmon resonance (SPR) spectroscopy, supplemented by AFM that provides the data on monolayer surface coverage of the peptide via direct imaging. Although QCM and SPR provided similar binding parameters, SPR provided a more detailed analysis of the adsorption process of 3R-GBP1. Here, we propose a biexponential kinetics to explain surface heterogeneity that possibly results in two different adsorption processes taking place simultaneously each with its own energy. The results indicate that 3R-GBP1 could be used as a molecular substrate, a potential alternative to thiols, in self-assembled molecular systems providing the added advantage of biocompatibility operating under aqueous (physiological) conditions.

Acknowledgment. This research was funded by grants from the U.S. Army Research Office, through the DURINT program (Defense University Research Initiative on Nanotechnology), and from National Science Foundation, through the MRSEC Program. We thank Mr. Chris So and Dr. H. Fong (AFM) and Ms. W. Trent (QCM) for their technical help. E.E.O. wishes to thank T. O. Ogurtani of METU for valuable suggestions on the kinetics analysis.

LA0606897